A Section 508–conformant HTML version of this article is available at https://doi.org/10.1289/EHP11257.

Accumulation of Black Carbon Particles in Placenta, Cord Blood, and Childhood Urine in Association with the Intestinal Microbiome Diversity and Composition in Four- to Six-Year-Old Children in the ENVIRONAGE Birth Cohort

Thessa Van Pee,[1] Janneke Hogervorst,[1] Yinthe Dockx,[1] Katrien Witters,[1] Sofie Thijs,[1] Congrong Wang,[1] Eva Bongaerts,[1] Jonathan D. Van Hamme,[2] Jaco Vangronsveld,[1,3] Marcel Ameloot,[4] Jeroen Raes,[5,6] and Tim S. Nawrot[1,7]

[1]Centre for Environmental Sciences, Hasselt University, Diepenbeek, Belgium
[2]Department of Biological Sciences, Thompson Rivers University, Kamloops, British Columbia, Canada
[3]Department of Plant Physiology and Biophysics, Faculty of Biology and Biotechnology, Maria Curie-Skłodowska University, Lublin, Poland
[4]Biomedical Research Institute, Hasselt University, Diepenbeek, Belgium
[5]Department of Microbiology and Immunology, Rega Instituut, KU Leuven–University of Leuven, Leuven, Belgium
[6]Center for Microbiology, VIB, Leuven, Belgium
[7]Department of Public Health and Primary Care, Leuven University, Leuven, Belgium

Background: The gut microbiome plays an essential role in human health. Despite the link between air pollution exposure and various diseases, its association with the gut microbiome during susceptible life periods remains scarce.

Objectives: In this study, we examined the association between black carbon particles quantified in prenatal and postnatal biological matrices and bacterial richness and diversity measures, and bacterial families.

Methods: A total of 85 stool samples were collected from 4- to 6-y-old children enrolled in the ENVIRonmental influence ON early AGEing birth cohort. We performed 16S rRNA gene sequencing to calculate bacterial richness and diversity indices (Chao1 richness, Shannon diversity, and Simpson diversity) and the relative abundance of bacterial families. Black carbon particles were quantified via white light generation under femtosecond pulsed laser illumination in placental tissue and cord blood, employed as prenatal exposure biomarkers, and in urine, used as a post-natal exposure biomarker. We used robust multivariable-adjusted linear models to examine the associations between quantified black carbon loads and measures of richness (Chao1 index) and diversity (Shannon and Simpson indices), adjusting for parity, season of delivery, sequencing batch, age, sex, weight and height of the child, and maternal education. Additionally, we performed a differential relative abundance analysis of bacterial families with a correction for sampling fraction bias. Results are expressed as percentage difference for a doubling in black carbon loads with 95% confidence interval (CI).

Results: Two diversity indices were negatively associated with placental black carbon [Shannon: −4.38% (95% CI: −8.31%, −0.28%); Simpson: −0.90% (95% CI: −1.76%, −0.04%)], cord blood black carbon [Shannon: −3.38% (95% CI: −5.66%, −0.84%); Simpson: −0.91 (95% CI: −1.66%, −0.16%)], and urinary black carbon [Shannon: −3.39% (95% CI: −5.77%, −0.94%); Simpson: −0.89% (95% CI: −1.37%, −0.40%)]. The explained variance of black carbon on the above indices varied from 6.1% to 16.6%. No statistically significant associations were found between black carbon load and the Chao1 richness index. After multiple testing correction, placental black carbon was negatively associated with relative abundance of the bacterial families *Defluviitaleaceae* and *Marinifilaceae*, and urinary black carbon with *Christensenellaceae* and *Coriobacteriaceae*; associations with cord blood black carbon were not statistically significant after correction.

Conclusion: Black carbon particles quantified in prenatal and postnatal biological matrices were associated with the composition and diversity of the childhood intestinal microbiome. These findings address the influential role of exposure to air pollution during pregnancy and early life in human health. https://doi.org/10.1289/EHP11257

Introduction

Ambient air pollution accounts for over 4.2 million premature deaths each year and is recognized as the most important environmental cause of disease.[1] The EU Directive 2008/50/EC states that there is no identifiable threshold for exposure to particulate matter (PM) with an aerodynamic diameter ≤2.5 μm ($PM_{2.5}$) below which it is not harmful to human health.[2] One of the most toxic components of $PM_{2.5}$ is believed to be combustion-derived PM, including black carbon particles, which are formed during incomplete fuel combustion and to which hazardous substances, such as heavy metals and polycyclic aromatic hydrocarbons (PAHs), can bind.[3,4] After inhalation, black carbon particles smaller than 1 μm can bypass the lung–blood barrier[5] and translocate to distal body sites, as substantiated by their presence in urine,[6] placental tissue,[7] and cord blood.[8] Quantified black carbon loads in these biological matrices correlate well with modeled prenatal and postnatal air pollution exposure and are therefore employed as individual internal exposure biomarkers.[6–8]

The human gut microbiome comprises 10–100 trillion symbiotic microbial cells,[9] mainly belonging to the bacterial phyla Firmicutes and Bacteroidetes.[10] The gut microbiome evolves during infancy to reach an adultlike state at approximately 3 y of life.[11] During early life, bacteria are indispensable for, among other things, shaping the host immune system and mucosal integrity.[12] Later on, the microbiome sustains human health via processes such as energy production and guardianship against pathogen colonization.[12,13] Therefore, a healthy indigenous bacterial microbiome is essential, and intestinal dysbiosis, i.e., bacterial community composition imbalance, has been implicated in the pathogenesis of several disorders, including diabetes,[14] obesity,[15] cognitive deficits,[16] and hypertension.[17] As such, investigating factors that alter intestinal bacterial richness and diversity is paramount. Diet, medication, socioeconomic status, and sex are well-known determinants.[18–20] Yet, these factors were calculated to explain in total 16% of the interindividual variation in intestinal bacterial composition, implying that over 80% of the variation remains unexplained.[21] These

Address correspondence to Tim Nawrot, Agoralaan building D, 3590, Diepenbeek, Belgium. Telephone: +3211268382. Email: tim.nawrot@uhasselt.be

Supplemental Material is available online (https://doi.org/10.1289/EHP11257).

M.A. and T.S.N. declare competing financial interests: Aspects of the work mentioned in the paper are the subject of a patent application (Method for detecting and quantifying black carbon particles, US20190025215A1) filed by Hasselt University (Hasselt, Belgium) and KU Leuven (Leuven, Belgium). The remaining authors declare no competing interests.

Received 15 March 2022; Revised 28 November 2022; Accepted 22 December 2022; Published 31 January 2023.

Note to readers with disabilities: *EHP* strives to ensure that all journal content is accessible to all readers. However, some figures and Supplemental Material published in *EHP* articles may not conform to 508 standards due to the complexity of the information being presented. If you need assistance accessing journal content, please contact ehpsubmissions@niehs.nih.gov. Our staff will work with you to assess and meet your accessibility needs within 3 working days.

findings suggest that additional factors, e.g., environmental factors like air pollution exposure, might play a role.

Studies addressing the impact of air pollution on the microbiome are scarce. Various animal studies found negative associations between air pollution exposure and the intestinal microbiome as summarized by Vallès et al.[22] Human studies exist as well: Mariani et al.[23] examined the impact of short-term PM exposure in adults on the nasal microbiome and found inverse associations with alpha diversity indices. A study[24] involving 8-y-old primary school children with asthma in China reported that 5-d smog exposure was associated with a decrease in the relative abundance of the fecal bacterial families *Bifidobacteriaceae* and *Erypsipelotrichaceae* and an increase in *Streptococcaceae*, *Rikenellaceae*, and *Porphyromonadaceae*. Prior-year residential concentrations of freeway traffic-related air pollution were linked to a decrease in the relative abundance of *Bacteroidaceae* and an increase in *Coriobacteriaceae* in the feces of 17- to 19-y-old overweight and obese U.S. adolescents.[25] A study[26] in type 2 adults with diabetes with an average age of 52 y found negative associations of the prior 2-y average residential $PM_{2.5}$ and PM_{10} exposure with alpha diversity indices of fecal microbiota. Together, the above studies suggest an influence of air pollution exposure on the gut bacterial diversity and composition.

Despite the emerging evidence, the effects of air pollution exposure on the gut microbiota in healthy children during susceptible life periods, i.e., fetal development and early childhood, remain uninvestigated. Here, we present a study within the ENVIR*ON*AGE birth cohort framework (ENVIRonmental influence ON early AGEing),[27] where we examined the association of air pollution with fecal bacterial richness and diversity, and the relative abundance of bacterial taxa. The primary objective was to investigate whether the placental and cord blood black carbon load (prenatal exposure biomarker) and urinary black carbon load (postnatal exposure biomarker) were associated with fecal bacterial richness and diversity in 4- to 6-y-old children.

Material and Methods

Study Population

The ENVIR*ON*AGE birth cohort recruits mother–newborn pairs at arrival for delivery in the East Limburg Hospital (ZOL; Genk, Belgium) and follows them longitudinally.[27] In total, 1,596 mother–child pairs are included in the cohort, and recruitment still continues. Written informed consent is obtained from all participating mothers, and the study is approved by the Ethical Committees of Hasselt University and East-Limburg Hospital (EudraCT B37120107805) and complies with the Helsinki Declaration. At the first antenatal visit, maternal body mass index (BMI) was determined by dividing the measured weight in kilograms by the measured height in square meters. The conception date was estimated based on the first day of the mother's last menstrual period combined with the first ultrasonographic examination. After delivery, detailed lifestyle and sociodemographic information about the mother and child were gathered via questionnaires (e.g., maternal age and education, parity, descent, smoking habits, and antibiotic use during pregnancy) and medical records (e.g., newborn sex, mode of delivery, and day of delivery). Parity was categorized as mothers having their first, second, or third or more child. Descent was classified as European when two or more grandparents were of European descent. Maternal education was coded as "low" when the mother did not obtain a high school diploma, "middle" when the mother obtained a high school diploma, and "high" when the mother obtained a college or university degree.[28] After approximately 4 and 10 y, mother–child pairs are contacted again to participate in the follow-up phase, in which anthropometric, cognitive, and cardiovascular examinations are performed and questionnaires regarding lifestyle, use of medication, and behavior are administered. In addition, a nonquantitative food frequency questionnaire detailing the child's daily intake of, e.g., fruit, vegetable, and soda consumption over the prior 3 months (never, <1 d/wk, 1 d/wk, 2 d/wk, 3–4 d/wk, 5–6/d/wk, one time per day, multiple times per day) is filled in by the mother.

For this study, mother–child pairs were contacted when the child reached the age of 4 to 6 y and were asked to agree to a house visit by a study employee, in which, among other biological samples and measurements, a stool and urine sample were collected from the child. In addition, questionnaire data (e.g., child's age, antibiotic use in the month before the house visit, in-house smoking, and maternal occupation) was gathered, and the child's anthropometrics (height and weight) were measured. Maternal occupational levels were coded using the Standard Occupational Classification: sales and customer service occupations, process, plant and machine operatives, and elementary occupations were coded as "low"; administrative and secretarial occupations, skilled trades occupations, and caring, leisure, and other service were coded as "middle"; and managers, directors, senior officials, professional occupations and associate professional and technical occupations were coded as "high."[29] Last, based on the home address of the mothers, median annual neighborhood income was defined using Belgian census-tract data (FOD Economie/DG Statistiek) as previously described.[29] Written informed consent was obtained from the parents and oral permission from the child at the start of the house visit. Participant recruitment was carried out in two phases: spring 2017 and spring 2018. For this study, only mother–child pairs who already participated in the 4-y follow-up study up to 1 y before the house visit or who were going to participate within 1 y after the house visit, mother–child pairs who did not (plan to) move between the house visit study and the 4-y follow-up study, and mother–child pairs who had no major renovations planned during the house visit study, were eligible for inclusion. In total, 284 eligible mother–child pairs were identified, of which we succeeded in contacting 233, and 157 agreed to participate in the house visit study, where 96 children provided a stool sample (success rate of stool sample collection was 61.1%). The main reasons that participants did not provide a stool sample were the collection of a stool sample within a limited time frame (only 2 d) and the "yuck factor." Three stool samples were excluded due to improper storage, four samples because of an insufficient DNA quality, and four due to a too-low number of sequence reads. As a result, the number of included participants amounted to 85, of which 36 (42%) were recruited in 2017 and 49 (58%) in 2018. Among the 85 participants, 63 participants had placental tissue, whereas cord blood and urine were each available from 80 participants (Figure 1). The overlap in availability for the three biological samples is depicted in Figure S1.

Sample Collection and Processing

At birth, fresh placental tissue was collected within 10 min after delivery. Four biopsies were taken at standardized sites: one in each quadrant of the fetal side across the middle region of the placenta, approximately 4 cm away from the umbilical cord and 1 cm below the chorion-amniotic membrane to avoid membrane contamination. Biopsies were stored at −80°C until further use.[30] Because a previous study showed no differences in black carbon load among the four biopsies in three women in this cohort, only one biopsy was used for further examination within this study.[7] For black carbon quantification, frozen biopsies were fixed in 4% formaldehyde on ice at least 24 h before being dehydrated and paraffin-embedded.[7] Additionally, 4-µm sections were cut using a microtome (Leica Microsystems) and mounted on histological glass slides. Per biopsy, five slides were prepared. Umbilical cord

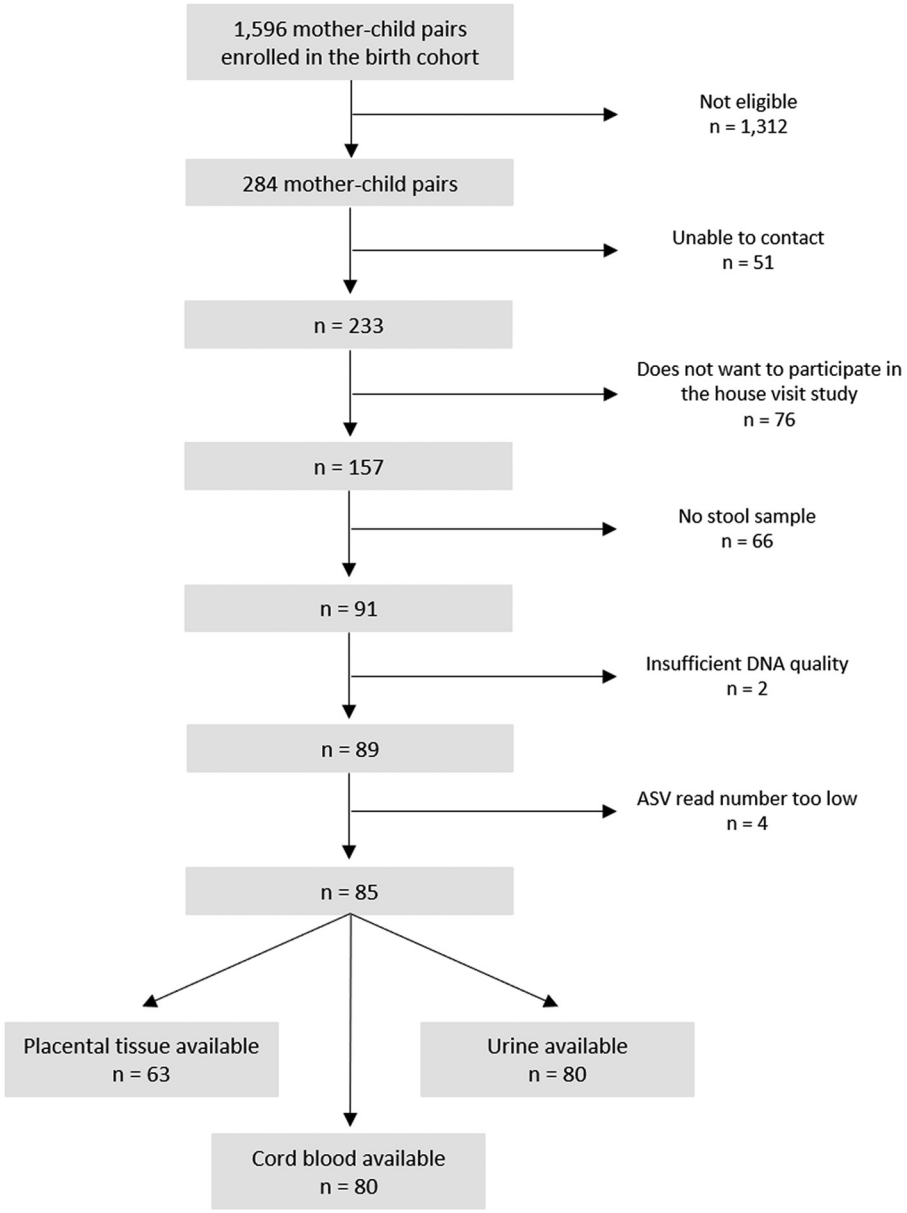

Figure 1. Participant flow chart depicting the selection of participants enrolled in the ENVIR*ON*AGE birth cohort for arriving at the final study sample size. Note: Only mother–child pairs who already participated in the 4-y follow-up study up to 1 y before the house visit or who were going to participate within 1 y after the house visit, mother–child pairs who did not (plan to) move between the house visit study and the 4-y follow-up study and who had no major renovations planned during the house visit study were eligible for inclusion in this study. ASV, amplicon sequence variant; ENVIR*ON*AGE, ENVIRonmental influence ON early AGEing birth cohort.

blood was also gathered within 10 min after delivery in BD Vacutainer plastic whole blood tubes, spray-coated with K_2 EDTA (BD) and stored at −25°C.[31] For black carbon measurements, cord blood samples were thawed at room temperature, vortexed (VWR International), and 100 µL was pipetted into imaging chambers fabricated in-house.[8] Two imaging chambers were prepared per participant. Imaging chambers were constructed by placing a glass coverslip (24 × 24 mm; no. 1.5, VWR) on a microscopic glass slide (75 × 25 mm; VWR) merged with 100 µm thick double-sided tape (product no. 4959, Tesa SE). The imaging chambers were air-sealed to prevent drying.

Two days before the house visit, the parent(s) collected one stool sample from their child in a designated sterile stool container (VWR) and stored it in their home freezer at −20°C. At the day of the house visit, the parent(s) also collected a urine sample and kept it in the refrigerator. After the examinations, stool and urine samples were taken, transported on ice, and stored at −80°C and −25°C, respectively, until further analysis. For black carbon analysis, urine aliquots were thawed on ice, homogenized for 30 min in a thermomixer (Eppendorf SE) at room temperature, and 100 µL was pipetted into the imaging chambers fabricated in-house (described above). Urinary osmolality was determined using 150 µL urine and a Knauer Osmometer (K-7400S) (Knauer).

Black Carbon Measurements

Black carbon particles were quantified in placental tissue, cord blood, and urine using white light generation under femtosecond pulsed illumination, allowing label-free detection.[32] All images of cord blood were gathered at room temperature using a Zeiss LSM880 NLO scan head mounted to the rear port of an inverted laser-scanning microscope (Zeiss Axio Observer.Z1 motorized

stand; Carl Zeiss) equipped with a two-photon femtosecond pulsed laser (810 nm, 120 fs, 80 MHz, MaiTai DeepSee; SpectraPhysics) and an Plan-ApoChromat 20×/0.8 M27 air objective (Carl Zeiss). All images of placental tissue and urine were collected at room temperature using a Zeiss LMS510 META NLO scan head mounted on an inverted laser-scanning microscope (Zeiss Axiovert 200M; Carl Zeiss) equipped with the same ultrashort pulsed laser using a Plan-Neofluar 10× per 0.3 M27 air objective for placental tissue and an EC Plan Neofluar 20× per 0.5 objective for urine (Carl Zeiss). For placental tissue, five 4-μm-thick sections were imaged entirely. The field view of the resulting tile scans ranged between 2,700×2,700 μm^2 and 4,500×4,500 μm^2, depending on the size of our tissue. This approach corresponds to either 9 images with a 3,888×3,888 pixel resolution or 25 images with a 6,480×6,480 pixel resolution, both recorded with a 2.51 μs pixel dwell time. For cord blood, the resulting tile scans had a field of view of 4,250.96×4,250.96 μm^2 containing 100 images with a 5,120×5,120 pixel resolution, recorded with a 1.54 μs pixel dwell time at three different locations within two imaging chambers. For urine, the resulting tile scans had a field of view of containing 9 images with a 1,536×1,536 pixel resolution and were recorded with a 1,60 μs pixel dwell time at five different locations in the imaging chamber. Cord blood and urine images were taken 5 μm above the coverslip.

For each image, two emission channels were employed (i.e., 450–650 nm for channel 1, and 400–410 nm for channel 2). In each channel, the number of black carbon particles was calculated using a peak-finding algorithm in MATLAB (MATLAB 2010; MathWorks, Inc.). This program counts pixels above a certain threshold value, i.e., 0.5% and 45% lower than the highest intensity value of channel 1 and channel 2, respectively. The detected pixels in both channels are compared, and only the matching pixels are identified as black carbon particle. For placental tissue, the effectively imaged placental area was determined in the imaging originating from channel 1 using Fiji (ImageJ). Based on MATLAB and Fiji outputs, the total relative number of black carbon particles per cubic nanometer of tissue or mL fluid was defined. We calculated Pearson correlation coefficients to assess the correlation between placental, cord blood, and urinary black carbon loads. In addition, to examine whether the measured black carbon load reflected well the participants' exposure to ambient airborne black carbon, we also calculated Pearson correlation coefficients between the measured and modeled data. Placental and cord blood black carbon loads were compared with ambient airborne black carbon exposure averaged over pregnancy. Similarly, the urinary black carbon load was correlated to the average airborne black carbon exposure over the month, 6 months, and year preceding the house visit. Modeled air pollution data was generated as follows: residential black carbon exposure levels (micrograms per cubic meter) were interpolated for each mother's (during pregnancy) and each child's (during early life) residential address using a spatiotemporal interpolation method that considers land-cover data obtained from satellite images (CORINE land-cover data set) and pollution data from fixed monitoring stations in combination with a dispersion model. This model provides daily interpolated exposure values in a high-resolution receptor grid using data from the Belgian telemetric air quality networks, point sources, and line sources. Overall model performance was evaluated by leave-one-out cross-validation including 14 monitoring points for black carbon, resulting in a spatiotemporal explanatory variance of over 74% in Flanders.[33] Daily air pollutants concentrations during pregnancy and the year preceding the house visit, taking into account address changes, were calculated.[27]

Intestinal Microbiome 16S rRNA V3-V4 Amplicon Sequencing

Stool samples were used as a proxy for the gut microbiome.[34] Bacterial DNA was extracted from 200 mg of stool employing the E.Z.N.A. Stool DNA Kit (Omega Bio-Tek Inc.) according to the manufacturer's instructions. The extracted DNA was eluted in an elution buffer (10 mM Tris/HCl, pH 8.5) and stored at −20°C after checking the quantity and quality spectrophotometrically (Nanodrop ND-1000 Spectrophotometer; Isogen Life Sciences). Due to insufficient DNA quality, four samples were omitted from further analysis.

Amplification of 16S rRNA Amplicon and Preparation of 16S Library

The bacterial V3-V4 16S rRNA gene region was amplified using primers that incorporate Ion Torrent sequencing adaptors and Ion Xpress barcodes [amplification PCR: 341F (5′-TAC GGG AGG CAG CAG-3′) and 806R (5′-GGA CTA CVS GGG TAT CTA AT-3′) primers (Alpha DNA); index PCR: sequencing adaptor (underlined, underlined and bold) Ion Xpress barcoded (bold) 341F (5′-CCA TCT CAT CCC TGC GTG TCT CCG ACT CAG **CTA AGG TAA CGA T**TA CGG GAG GCA GCA G-3′) with P1 (underlined) adapted 806R (5′-CCA CTA CGC CTC CGC TTT CCT CTC TAT GGG CAG TCG GTG ATG GAC TAC VSG GGT ATC TAA T-3′)]. Both amplicon and index amplification were achieved on a T100 Thermal Cycler (Bio-Rad) via the polymerase chain reaction (PCR) programs in the Tables S1, S2, and S3. Amplified products from each round were purified using AMPure XP beads (Beckman Coulter) and a magnetic rack, quantified with the Quant-iT dsDNA HS Assay Kit (Thermo Fisher Scientific), and visualized on agarose gels (1.5% agarose gel, 1.5h, 90V). Barcoded amplicons were pooled in equimolar amounts, and the library dilution factor was determined using an Ion Library Quantitation Kit. An Ion 510 & 520 & 530 Kit-Chef on an Ion Chef system was used for sequencing template preparation, and sequencing was performed on an Ion 530 chip using 400 bp paired-end chemistry.

Sequencing Data Analysis

Sequencing data were received as a set of Ion Torrent-sequenced FASTQ files. Sequences were demultiplexed using the Ion Torrent software, and subsequently underwent quality trimming and primers removing using DADA2 1.10.1.[35] Parameters for length trimming were set to keep the first 230 bases of the forward read, maxN = 0, MaxEE = (2), trimLeft = 15, and truncQ = 2. Reads were de-replicated and error rates were inferred using the DADA2 default parameters. Sequence variants were inferred using the adjusted parameters for Ion Torrent-sequences: dada (homopolymer_gap_penalty = −1, band_size = 32). After removal of chimeras via the removeBimeraDenovo() function, an amplicon sequence variant (ASV) table was built and taxonomy assigned using the assignTaxonomy function and the SILVA v138 training set,[36,37] and alternatively using DECIPHER[38] for taxonomic classification with IDTaxa function and the SILVA_SSU_r138_2019 database. The resulting ASVs and taxonomy tables were combined with the metadata file into a phyloseq object (Phyloseq, version 1.26.1).[39] Contaminants were removed from the dataset using the package Decontam (version 1.2.1), applying the prevalence method with a 0.5 threshold value.[40] Four samples were omitted from the analyses due to an insufficient number of reads (<10,000). Relative taxa abundances at family level were computed by normalizing the number of sequencing reads per ASV for the overall number of sequencing reads per stool sample. The relative abundance of a bacterial family thus represents what percentage (ranging from 0% to

Table 1. Anthropometric and lifestyle characteristics of the participating mother–child pairs ($n = 85$) enrolled in the ENVIR*ON*AGE birth cohort.

Characteristics	Participants ($n = 85$)	
	Median ± IQR	Total number (%)
Child characteristics		
Sex	—	—
Male	—	40 (47.1%)
Female	—	45 (52.9%)
Age (y)	4.8 ± 0.8	—
Weight (kg)	18.3 ± 3.0	—
Height (cm)	107.0 ± 6.8	—
Descent	—	—
European	—	82 (96.5%)
Non-European	—	3 (3.5%)
Gestational duration (d)	280.0 ± 11.0	—
Season of delivery	—	—
Winter	—	23 (27.1%)
Spring	—	13 (16.5%)
Summer	—	24 (28.2%)
Autumn	—	24 (28.2%)
Antibiotic use in the month before sample collection	—	—
No	—	77 (90.6%)
Yes	—	8 (9.4%)
In-house smoke exposure	—	—
No	—	83 (97.6%)
Yes	—	2 (2.4%)
Vegetable intake[a]	—	—
Never	—	0 (0%)
<1 d/wk	—	1 (1.4%)
1 d/wk	—	1 (1.4%)
2 d/wk	—	1 (1.4%)
3–4 d/wk	—	8 (10.8%)
5–6 d/wk	—	14 (18.9%)
1 time/d	—	40 (54.1%)
Multiple times/d	—	9 (12.2%)
Fruit intake[a]	—	—
Never	—	1 (1.4%)
<1 d/wk	—	0 (0%)
1 d/wk	—	2 (2.7%)
2 d/wk	—	2 (2.7%)
3–4 d/wk	—	10 (13.5%)
5–6 d/wk	—	8 (10.8%)
1 time/d	—	23 (31.1%)
Multiple times/d	—	28 (37.8%)
Soda intake[a]	—	—
Never	—	31 (41.9%)
<1 d/wk	—	15 (20.3%)
1 d/wk	—	9 (12.2%)
2 d/wk	—	7 (9.5%)
3–4 d/wk	—	3 (4.1%)
5–6 d/wk	—	1 (1.4%)
1 time/d	—	8 (10.8%)
Multiple times/d	—	0 (0%)
Mother Characteristics		
Age at delivery (y)	30.0 ± 5.0	—
BMI (kg/m^2)	22.6 ± 3.7	—
Smoking during pregnancy	—	—
No	—	79 (92.9%)
Yes	—	6 (7.1%)
Antibiotic use during pregnancy	—	—
No	—	74 (87.1%)
Yes	—	11 (12.9%)
Parity	—	—
First child	—	44 (51.8%)
Second child	—	34 (40.0%)
Third or following child	—	7 (8.2%)
Education level	—	—
Low	—	2 (2.4%)
Middle	—	23 (27.1%)
High	—	60 (70.5%)
Occupation level	—	—
Low	—	9 (10.6%)
Middle	—	32 (37.6%)
High	—	44 (51.8%)
Median annual neighborhood income (Euro)	25,981.4 ± 4,011.8	—
Mode of delivery	—	—
Vaginal	—	84 (98.8%)
Cesarean section	—	1 (1.2%)

Note: Continuous covariables are expressed as median ± IQR and categorical covariables are described as total number (n) and percentage (%). Maternal educational level was coded "low" if the participant did not obtain a high school diploma, "middle" if the participant obtained a high school diploma, and "high" if the participant obtained a college or university degree. Maternal occupational levels were coded using the Standard Occupational Classification: sales and customer service occupations, process, plant and machine operatives, and elementary occupations were coded "low"; administrative and secretarial occupations, skilled trades occupations and caring, leisure and other service were coded "middle"; and managers, directors, senior officials, professional occupations and associate professional and technical occupations were coded "high." Descent was based on the native country of the newborn's grandparents and described as European when two or more grandparents were European, or non-European when at least three grandparents were of non-European origin. —, no data; BMI, body mass index; ENVIR*ON*AGE, ENVIRonmental influence *ON* early AGEing birth cohort; IQR, interquartile range.
[a]Data available for 74 participants.

100%) of the microbiome that is made up of that specific family. In a log-log model, a percentage change of, e.g., 235% per doubling in exposure would mean a 2.35-fold increase. Rarefaction analysis was performed with ranacapa 0.1.0.[41] Based on the ASV table, alpha diversity was assessed by calculating Chao1 richness index, Shannon diversity index, and Simpson diversity index. Chao1 richness estimates the total richness, i.e., the number of expected species, based on the number of observed species, considering that low abundance species might be missed. In addition, Shannon and Simpson diversity take into account both richness and evenness. The Shannon diversity index focuses most on species richness and reflects the degree of uncertainty in predicting where randomly selected species will belong and ranges from one (single dominant specie) to the total number of all species (all species having equal abundance). A larger value indicates a greater diversity. On the other hand, the Simpson diversity index places greater emphasis on species evenness and ranges between 0 and 1. It reflects the probability that two bacteria randomly selected will belong to different species; hence, a larger value reflects a greater diversity.[42]

Statistical Analyses

All statistical analyses were performed using R Statistical Software (version 4.0.5; R Foundation for Statistical Computing). Descriptive statistics of the lifestyle characteristics are presented in Table 1 for all included participants ($n = 85$) and compared to the entire birth cohort (Table S4). Continuous variables are expressed as median ± interquartile range (IQR) and categorical variables as total number (n) and percentage (%). To improve normality of the distributions, we log-transformed black carbon loads and richness and diversity indices. First, robust linear regression models were fitted between the modeled black carbon exposure data (i.e., exposure during pregnancy and the month, 6 months, and year before stool sample collection) and the Chao1 richness, Shannon diversity and Simpson diversity indices, while accounting for the following covariables based on previous associations between the covariable and either the fecal microbiome or air pollution: parity (first, second, or third and more),[43] season of delivery (winter, spring, summer, or autumn),[44] sequencing batch (first or second),[45] child's age (continuous),[46] sex (male or female),[47] weight (continuous),[48] height (continuous),[49] and maternal education

(low, middle, or high)[20,50] as a proxy for socioeconomic status.[51–53] Afterward, (Partial) Spearman correlations coefficients (r) and coefficients of determination (R^2) were calculated to evaluate the correlations between the different richness and diversity indices and black carbon loads while accounting for the same covariables. Subsequently, the standardized R^2 values of black carbon loads were compared to the standardized R^2 values of other covariables.

Next, robust multiple linear regression models were fitted to assess the effect size of black carbon loads in placental tissue, cord blood, and urine on the Chao1 richness index, Shannon diversity index, and Simpson diversity index, respectively, while accounting for the same covariables. A multiexposure robust linear regression model incorporating both prenatal (cord blood black carbon) and postnatal (urinary black carbon) exposure was fitted to assess the relative effect size on each of the richness and diversity indices. This multiexposure model was also adjusted for the aforementioned covariables. Cord blood black carbon was employed as prenatal exposure biomarker since cord blood samples were available for a larger number of participants compared to placental tissue. Robust models and partial correlations were used because of the small sample size to reduce the effect of influential cases. Results are presented as a percentage change (%) in index for a doubling in black carbon load. In a sensitivity analysis, we assessed whether the mode of delivery (vaginal or cesarean section),[54] smoking during pregnancy (yes or no),[55] antibiotic use during pregnancy (yes or no),[56] in-house smoking during childhood (yes or no),[57] antibiotic use in the child during the month before stool sampling (yes or no),[58] descent (European or non-European),[59] BMI z-score (continuous) instead of weight and height separately,[60] fruit, vegetables, and soda intake as proxies for diet (never, <1 d/wk, 1 d/wk, 2 d/wk, 3–4 d/wk, 5–6 d/wk, one time per day, multiple times per day),[61] maternal occupation (low, middle, high)[26] instead of maternal education, or adjustment for neighborhood income (continuous)[62] together with maternal education affected the observed associations between the diversity measures and black carbon loads. Last, raw family counts were used to perform a differential relative abundance analysis at the family level using the "Analysis of Compositions of Microbiomes with Bias Correction" (ANCOM-BC) R package (version 1.0.55).[63] Multiple testing was corrected by restricting the false discovery rate as lower than 0.10. All other options remained as default. All reported p-values were two-tailed and a $p \leq 0.5$ was used to define statistical significance.

Results

Population Characteristics

Table 1 shows the anthropometric and lifestyle characteristics of the participating mother–child pairs. In total, 85 children were included, of which almost half were male (47%). On average ± IQR, children were 5 ± 1 y of age with a mean weight of 18 ± 3 kg and mean height of 107 ± 7 cm. Almost all of them were of European descent (97%), and half of them were the first-born (52%). Eight children (9%) took antibiotics in the month before stool sample collection, whereas only two (2%) were exposed to in-house smoke. Most children ate vegetables once a day (54%), ate fruit multiple times a day (39%), and never drank soda (42%). The average ± IQR maternal age at delivery was 30 ± 5 y, with a mean prepregnancy BMI of 23 ± 4 kg/m^2. The gestational duration was on average ± IQR 280 ± 11 d, with 23 children born in winter (27%), 13 children in spring (17%), 24 children in summer (28%), and 24 children in autumn (28%). Only one mother gave birth via a cesarean section (1%). Six mothers (7%) smoked during pregnancy, and 11 mothers (13%) took antibiotics. Most mothers obtained a college or university degree (71%) and had an occupation classified as middle or high using the Standard Occupational Classification (89%). The average median annual neighborhood income was approximately 26,000 ± 4,000 Euro.

Black Carbon Measurements in Biological Matrices and Modeled Values

Black carbon particles were identified in all three biological matrices (Figure 2). The median ± IQR loads in placental tissue, cord blood, and urine were $2.25 \times 10^4 \pm 1.25 \times 10^4$ particles per cubic millimeter tissue, $5.80 \times 10^4 \pm 2.82 \times 10^4$ particles per milliliter cord blood, and $1.58 \times 10^5 \pm 1.16 \times 10^5$ particles per milliliter urine, respectively (Table 2). Pearson correlation coefficients were calculated between the black carbon values in the three biological matrices: at birth, placental and cord blood black carbon were positively correlated ($r = 0.39$, $p = 0.002$), whereas no significant correlations were observed between black carbon in placenta or cord blood at birth and urine sampled 4 y later ($r = 0.23$, $p = 0.10$; $r = 0.09$, $p = 0.44$, respectively). In addition to black carbon measurements, modeled air pollution values were also employed. The median ± IQR modeled black carbon exposure during pregnancy and the month, 6 months, and year preceding the house visit study were 0.89 ± 0.32 μg/m^3, 0.70 ± 0.23 μg/m^3, 0.99 ± 0.18 μg/m^3, and 0.96 ± 0.20 μg/m^3, respectively. We found that the modeled black carbon exposure during pregnancy was significantly correlated with black carbon particles quantified in placental tissue ($r = 0.48$, $p < 0.0001$) and cord blood ($r = 0.44$, $p < 0.0001$). Modeled black carbon exposure in the month, 6 months, and year preceding the house visit study were correlated with black carbon particles quantified in urine samples normalized for osmolality (month: $r = 0.32$, $p = 0.004$; 6 months: $r = 0.25$, $p = 0.03$; year: $r = 0.18$, $p = 0.11$) (Figure 3; Table S5).

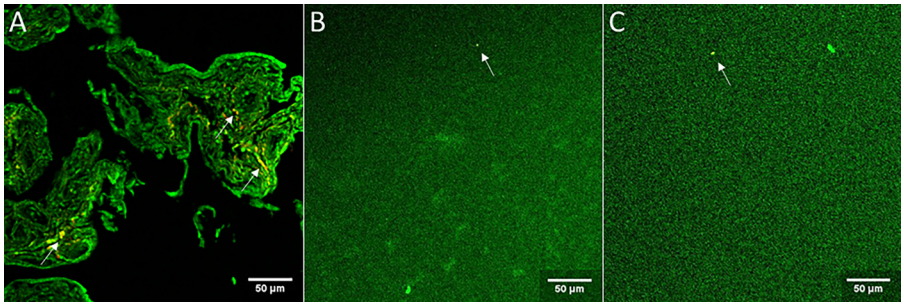

Figure 2. Evidence of black carbon particles in (A) placental tissue, (B) cord blood, and (C) urine. White light generation originating from black carbon particles (yellow, indicated with a white arrow) under femtosecond pulsed laser illumination (excitation 810 nm, 120 fs, 80 MHz) was observed. Images represent the overlap of channel 1 (green, emission 450–650 nm) and channel 2 (red, emission 400–410 nm). All samples were collected in the ENVIR*ON*AGE birth cohort and images were randomly selected from different participants. Scale bar: 50 μm. Note: ENVIRONAGE, ENVIRonmental influence ON early AGEing birth cohort.

Table 2. Detailed information on the distribution of the placental, cord blood, and urinary BC load, quantified via the white light technique.

	Placental BC load ($n=63$)	Cord blood BC load ($n=80$)	Urinary BC load ($n=80$)
Mean	22,488	58,041	177,731
Median	23,162	54,535	157,834
Standard deviation	8,733	25,211	116,419
25th percentile	15,875	42,849	92,171
75th percentile	28,410	71,090	234,356
Minimum value	5,208	11,686	426
Maximum value	44,788	151,919	539,538

Note: Samples were collected in the ENVIR*ON*AGE birth cohort framework: placental tissue and cord blood were collected at birth and urine during the house visit study. Placental BC load is expressed as number of particles per cubic millimeter tissue and cord blood and urinary BC load are expressed as number of particles per milliliter fluid. Urinary black carbon is normalized for osmolality. BC, black carbon; ENVIR*ON*AGE, ENVIRonmental influence *ON* early AGEing birth cohort.

Sequencing Data and Alpha Diversity of the Intestinal Microbiome

Sequence data of the 16s rRNA gene hypervariable V3-V4 region were analyzed to obtain a median ± IQR of 84,132 ± 95,725 reads per sample and a median ± IQR of 168 ± 87 ASVs. Rarefaction analysis indicated that all samples had been sufficiently sequenced (Figure S2). Bacterial relative abundance levels were calculated at the family level (Figure 4). The most dominant bacterial families were *Lachnospiraceae* (29%), *Bacteroidaceae* (23%), and *Ruminococcaceae* (18%), together accounting for approximately 70% of the total bacterial taxa abundance. *Lachnospiraceae* and *Ruminococcaceae* belong to the phylum Firmicutes, whereas *Bacteroidaceae* is part of the phylum Bacteroidetes. Next, fecal microbiome richness and diversity indices were calculated for each sample. The species-richness measure Chao1 had a median value ± IQR of 168 ± 87. The species-diversity measures Shannon and Simpson, which combine richness and evenness estimates, had a median value ± IQR of 3.8 ± 0.62 and 0.95 ± 0.03, respectively.

Association between Black Carbon Exposure/Loads and Intestinal Microbiome Alpha Diversity

Modeled exposure to black carbon particles during the entire pregnancy and the month, 6 months, or year prior to stool sample collection were not associated with the alpha diversity of the intestinal microbiome (Table S6).

Both before and after adjustment for parity, season of delivery, batch, child's age, sex, weight and height, and maternal education, significant negative correlations were observed between placental, cord blood, and urinary black carbon, and the Shannon and Simpson diversity indices (Figure 5; Table S7). Placental black carbon explained on average 13% of the variation in the Shannon and 17% of the variation in Simpson diversity indices. The explained variance of these indices by the black carbon load of cord blood were 6% and 8%, respectively, and by the urinary black carbon were 10% and 8%, respectively. Moreover, when comparing the standardized R^2 values of black carbon loads, we found that black carbon in all three biological matrices explained on average as much variation in the Shannon diversity index as antibiotic use during the previous month or soda intake during the previous 3 months, whereas the explained variance of black carbon on the Simpson diversity index was five times higher in comparison with the same two covariables (Figure 6; Table S8).

The robust multiple linear regression models confirmed our previous findings and evaluated the effect size of the association between black carbon loads and richness and diversity indices (Table 3). Overall, bacterial diversity indices Shannon and Simpson were inversely associated with both prenatal black carbon exposure (placental and cord blood black carbon) and postnatal exposure (black carbon load of urine). Each doubling in placental black carbon was associated with a 4.38% lower (95% CI: −8.31%, −0.28%; $p=0.04$) Shannon diversity index and a 0.90% lower (95% CI: −1.76%, −0.04%; $p=0.04$) Simpson diversity index. Each doubling in cord blood black carbon was associated with a 3.38% lower (95% CI: −5.66%, −0.84%; $p=0.05$) Shannon index, and a 0.91% lower (95% CI: −1.66%, −0.16%; $p=0.02$) Simpson diversity index. Last, for each doubling in urinary black carbon, the Shannon diversity index was 3.39% lower (95% CI: −5.77%, −0.94%; $p=0.009$), and the Simpson diversity index was 0.89% lower (95% CI: −1.37%, −0.40%; $p<0.0001$). No statistically significant associations were found in black carbon loads with the Chao1 richness index (Table 3). Additionally, the multiexposure model showed that each doubling in cord blood black carbon was associated with a 0.85% lower (95% CI: −1.59%, −0.10%; $p=0.03$) Simpson diversity index, whereas the association with the Shannon diversity index did not remain statistically significant (−2.61%, 95% CI: −6.17%, 1.10%; $p=0.16$). On the other hand, each doubling in urinary black carbon was associated with a 3.51% lower (95% CI: −5.95%, −1.00%; $p=0.006$) Shannon diversity index and a 1.05% lower (95% CI: −1.56%, −0.54%; $p<0.0001$) Simpson diversity index (Table 4).

In sensitivity analyses, we examined whether the main findings of the robust multiple linear regression models remained after correcting for smoking during pregnancy ($n=6$); antibiotic use during pregnancy ($n=11$); antibiotic use 1 month before stool sampling ($n=8$); BMI z-score instead of weight and height separately; fruit, vegetable, and soda intake (data available for 74 participants); maternal occupation instead of maternal education, or neighborhood income together with maternal education; or excluding children exposed to in-house smoke ($n=2$), mothers who gave birth via a cesarean section ($n=1$), or children of non-European descent ($n=3$). Correction for these variables or exclusion of these participants did not significantly change the effect estimates (Table S9).

Raw family counts were used as input to the ANCOM-BC R package to examine the relationship between black carbon loads and relative abundance at the family level (Table 5). Results are expressed as a percentage change in bacterial family per doubling in black carbon load. Within the model, we accounted for the same covariables that were accounted for in previous models. The associations between placental, cord blood, and urinary black carbon and all bacterial families are depicted in Table S10. After multiple testing correction via the false discovery rate, two bacterial families were inversely associated with placental black carbon, *Defluviitaleaceae* (−73.7%; $q=0.09$), *Marinifilaceae* (−96.9%; $q=0.08$), and two bacterial families were negatively associated with the urinary black carbon load: *Christensenellaceae* (−85.8%; $q=0.03$) and *Coriobacteriaceae* (−80.7%; $q=0.08$). The associations found with cord blood black carbon and bacterial families did not survive multiple testing.

Discussion

The key finding of our study is that the load of black carbon particles in prenatal tissues (placenta and cord blood) and in child urine was associated with lower fecal bacterial diversity and lower relative abundance of specific bacterial taxa in children age 4–6 y. Statistically significant negative correlations and associations were observed between the placental, cord blood, and urinary black carbon loads and the Shannon and Simpson diversity indices. High richness and diversity

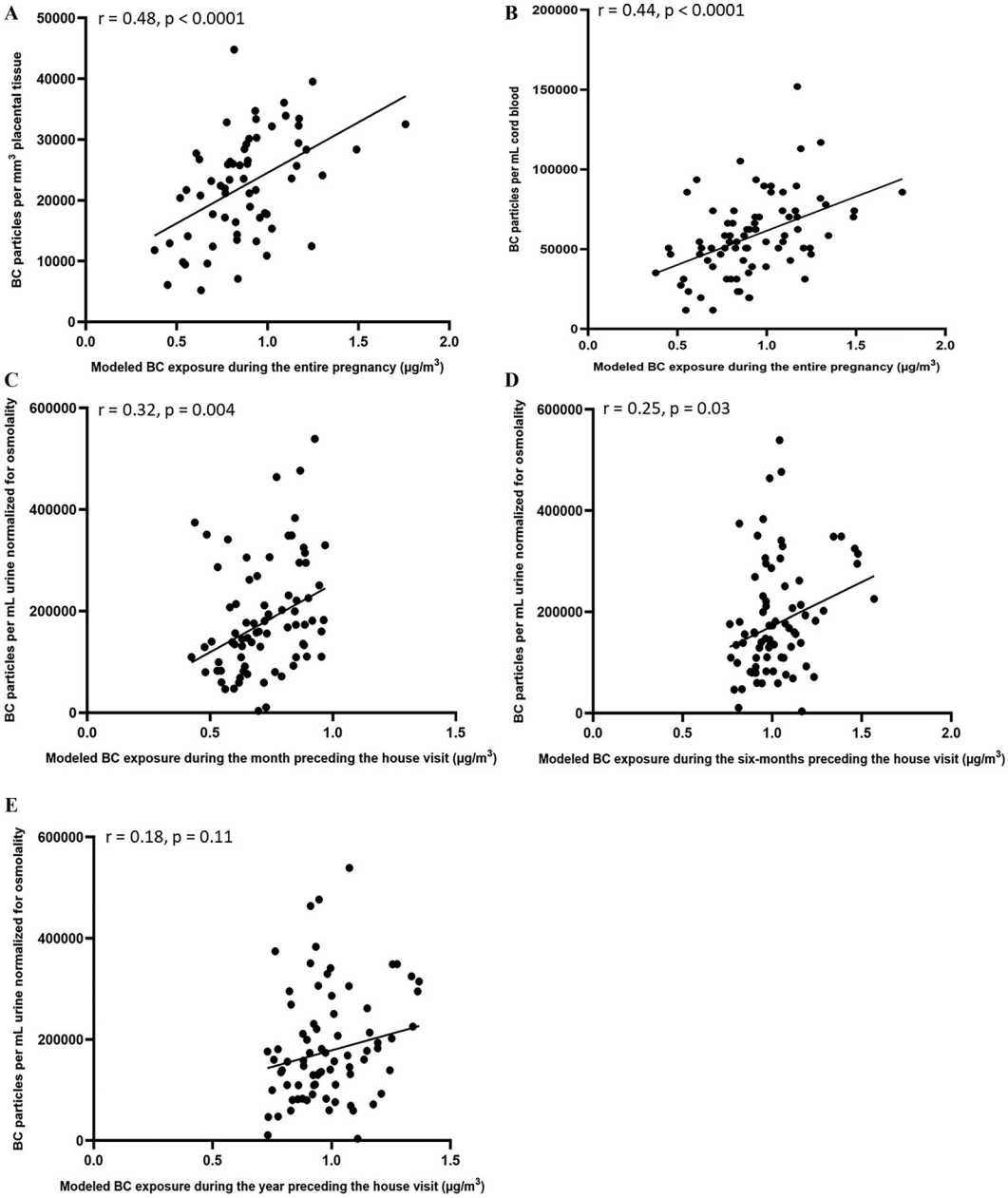

Figure 3. Correlation graphs between (A) placental black carbon and residential black carbon exposure averaged over the entire pregnancy ($n = 63$), (B) cord blood black carbon and residential black carbon exposure averaged over the entire pregnancy ($n = 80$), and (C), (D), and (E) urinary black carbon normalized for osmolality ($n = 80$) and residential black carbon exposure averaged over the (C) preceding month, (D) preceding 6 months, and (E) preceding year of the house visit. See Table S5 for corresponding numeric data. Participants are enrolled in the ENVIR*ON*AGE birth cohort. Note: ENVIR*ON*AGE, ENVIRonmental influence ON early AGEing birth cohort.

measures are important indicators of a healthy intestinal microbiome in humans, because a wide array of gut microbes are associated with a more capable and resilient gut microbiome, resulting in an improved health status.[53,64,65] If air pollution exposure lowers gut bacterial diversity indices, this exposure could have detrimental effects on gut health. Within this study, fecal samples were used as a proxy for the gut microbiome.[34] Our findings might have a public health impact because we found that between 6%–17% of the interindividual variation in intestinal bacterial composition at the species level could be explained by prenatal and postnatal measures of internal black carbon levels. To our knowledge, this is the first study that linked a measure of internal ambient air pollution particles with differences in the childhood gut microbiome. Furthermore, human studies examining the effect of prenatal air pollution exposure on the intestinal microbiome are lacking.

For every doubling in internal black carbon load in placental tissue, cord blood, and urine, the Shannon and Simpson indices decreased approximately 4% and 1%, respectively. Due to the large interindividual variation in black carbon load (e.g., ranging from 5,208 to 44,788 for placental black carbon), multiple doublings are necessary to compare doublings for low- and high-exposed children (e.g., four doublings to go from low- to high-exposed for placental black carbon). Thus, diversity indices differed considerably among low- and high-exposed participants. Additionally, other studies on the association between air pollution exposure and the intestinal microbiome did not find significant associations with bacterial diversity indices.[24,25] The findings of our study are in line

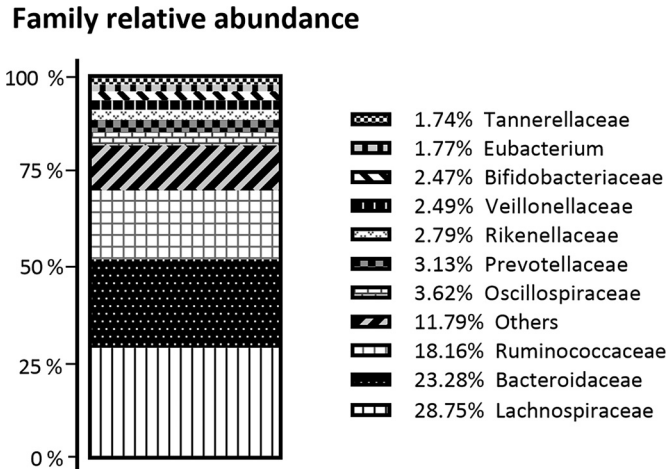

Figure 4. Overview of the relative abundance (percentage) of the 10 most abundant bacterial families in relation to all other taxa. Height of bars represents the relative abundance. Families are ranked in increasing order from bottom to top. Participants were enrolled in the ENVIR*ON*AGE birth cohort. $n = 85$. ENVIR*ON*AGE, ENVIRonmental influence ON early AGEing birth cohort.

with the results of a previous study[53] examining the effect of previous-year outdoor ozone (O_3) exposure on the fecal bacterial richness and diversity in 101 adolescents living in Southern California. They noted negative associations between O_3 exposure and bacterial evenness ($p < 0.001$) and the Shannon diversity index ($p < 0.001$) at the species level. They reported that up to 11.2% of the interindividual variation in bacterial composition at the species level could be explained by O_3 concentrations. Similarly, negative associations were observed between $PM_{2.5}$ and PM_{10} exposure during the preceding 3.5 y of life and intestinal alpha diversity of fecal samples in Chinese adults.[26]

In the current study, the bacterial families that negatively correlated with placental and urinary black carbon differed from each other. This differential suggests that prenatal and postnatal exposure to black carbon may exert different effects on the gut microbiome. An inverse association was observed between the placental black carbon load and the bacterial families *Defluviitaleaceae* and *Marinifilaceae* after correction for multiple testing. Both families have previously been linked to disorders, despite the lack of functional information. For instance, in a study by Liu et al.,[66] 64 patients with hyperlipidemia, which is characterized by elevated blood cholesterol and triglycerides levels and forms a major risk factor for coronary heart disease, ischemic stroke, and peripheral artery disease, were divided into two groups: group one, in which statin (a cholesterol-lowering medicine) treatment was successful, and group two, in which treatment failed. The relative abundance of the intestinal bacterial family *Defluviitaleaceae* was higher in men and women belonging to the first group in comparison with men and women in the second group. This finding suggests a modulating effect of *Defluviitaleaceae* on drug efficiency and accordingly the treatment of hyperlipidemia. Additionally, 41 inactive adults with celiac disease showed enriched intestinal *Defluviitaleaceae* levels accompanied by a reduction in resting heart rate after a 12-wk intervention with high-intensity interval training and lifestyle education.[67] Furthermore, the bacterial family *Marinifilaceae* was negatively associated with black carbon particles in placental tissue in this study. *Marinifilaceae* has been indicated as a key actor in gut health by Ge et al.[68] Specifically, mice on a high-fat diet received two hypoglycemic compounds to resolve their lipid metabolism disorder. After treatment, a statistically significant increase in the relative abundance of four intestinal bacterial families, including *Marinifilaceae*, was observed, linking this bacterium to a healthy intestinal flora. In addition, a study of the Cameron County Hispanic Cohort[69] ($n = 217$) in South Texas reported that the gut microbiome of Hispanic adults with liver fibrosis ($n = 28$) in comparison with healthy controls was enriched with immunogenic commensals and depleted of, among other bacterial families, *Marinifilaceae*.

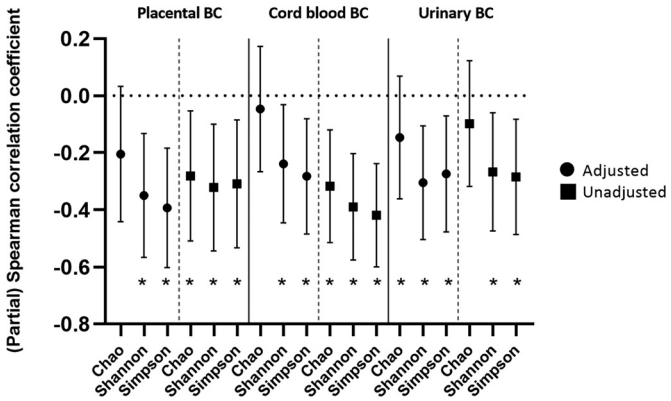

Figure 5. (Partial) Spearman correlation coefficients with 95% CI between Chao1 richness index, Shannon diversity index, and Simpson diversity index and placental black carbon load, cord blood black carbon, or urinary black carbon normalized for osmolality, based on corrected (partial/adjusted) and uncorrected models. Partial Spearman and adjusted coefficient of determination models were adjusted for parity, season of delivery, batch, age, sex, weight, height, and maternal education per categories included in Table 1. See Table S7 for corresponding numeric data. Participants were enrolled in the ENVIR*ON*AGE birth cohort. * indicates $p \leq 0.05$. p-Values were calculated using pairwise (partial) Spearman correlation. Placenta $n = 63$, cord blood $n = 80$, and urine $n = 80$. Note: BC, black carbon; CI, confidence interval; ENVIR*ON*AGE, ENVIRonmental influence ON early AGEing birth cohort.

Using urinary black carbon load to reflect childhood exposure, we found that a higher load was associated with a lower relative abundance of the bacterial families *Christensenellaceae* and *Coriobacteriaceae* after false discovery rate correction. Both *Christensenellaceae* and *Coriobacteriaceae* have been associated with gut health,[70] because patients suffering from Crohn's disease and ulcerative colitis have been reported to harbor significantly lower levels of them.[71–73] *Coriobacteriaceae* maintain host health by assisting in glucose, bile salt, and steroid metabolism and the activation of dietary polyphenols.[74–76] A study conducted by Zhao et al.[74] reported increased *Coriobacteriaceae* levels in stool samples in response to physical activity, whereas significantly lower levels were observed in mucosal–luminal interface samples from type two diabetes patients in comparison with healthy controls.[76] *Christensenellaceae* is also involved in metabolic health, as demonstrated by Goodrich et al.[77] and Fu et al.[78] They found negative correlations with BMI and low-density lipoproteins and positive correlations with high-density lipoproteins. Additionally, *Christensenellaceae* has been found to be depleted in individuals suffering from metabolic syndrome, characterized by visceral fat, dyslipidemia, impaired glucose metabolism, increased risk for type 2 diabetes, and cardiovascular disease.[79] Thus, higher intestinal *Christensenellaceae* levels have been linked to a lower cardiometabolic risk score.[70,79] Together, these studies highlight the importance of a stable, indigenous gut microbiome to maintain host health.

Prenatal and postnatal exposure to black carbon particles may influence intestinal bacterial growth via, among other mechanisms, systemic inflammation. Black carbon exposure has been associated with markers of systemic inflammation, e.g., increased white blood cell count and pro-inflammatory cytokines such as

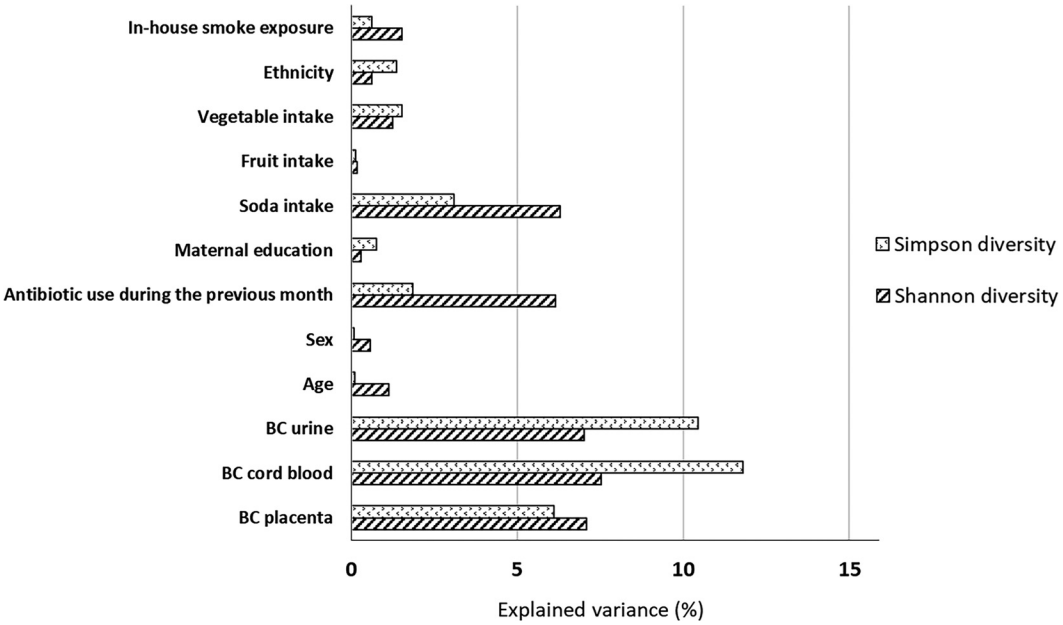

Figure 6. Percentage of variance (R^2) in Shannon or Simpson diversity explained by different covariables. Covariables were categorized as depicted in Table 1. See Table S8 for corresponding numeric data. Participants were enrolled in the ENVIR*ON*AGE birth cohort. Note: ENVIR*ON*AGE: ENVIRonmental influence ON early AGEing birth cohort.

interleukin-6, in both children[80] and adults,[81] including pregnant women. Subsequently, these pro-inflammatory mediators could impact intestinal bacterial growth, preferentially depleting beneficial gut flora and promoting the growth of otherwise dormant bacteria with potential pathogenic properties.[82–84] For instance, male C57BL/6j mice long-term intratracheally instilled with diesel exhaust particles had higher circulating levels of interleukin-1β in serum accompanied by a higher relative abundance of *Helicobacteraceae*, *Campylobacterales*, Campylobacteria, *Desulfovibrionaceae*, *Duslfovibrionales*, *Polyangiaceae*, Myxococcales, and Deltaproteobacteria and lower relative abundance of *Deferribacteraceae*, *Deferribacterales*, and Deferribacteres.[85] In addition, there may be a maternal–fetal efflux of pro-inflammatory mediators,[86] and therefore we hypothesize that inflammation could impact the child's gut microbiome in the womb. Prenatal black carbon exposure might also impact the gut microbiome via other pathways. For a long time, the "sterile womb paradigm" was an accepted dogma, stating that the human body is only colonized with microorganisms during and after birth.[87] Depending on the route of delivery, these pioneering microbes are predominantly of vaginal, cutaneous, or oral origin.[88,89] If air pollution exposure during pregnancy could influence the maternal vaginal, skin, and/or oral microbiome, this exposure might indirectly impact the infant's intestinal microbiome. In addition, maternal skin bacteria such as *Staphylococcus*, *Streptococcus*, *Lactobacillus*, and *Bifidobacterium* might also be transferred during breastfeeding.[90] Yet, recent studies challenged this dogma by discovering bacteria in placental tissue, amniotic fluid, and meconium.[91–93] This "*in utero* colonization theory" leaves open the possibility of a maternal–fetal efflux of commensal bacteria,[87] providing another framework of how prenatal air pollution exposure could more directly influence an infant's intestinal microbiome. However, the presence of bacteria in meconium samples is also debated, because studies[94,95] reported that the bacteria found in the majority of the "dogma-challenging" studies originated from contamination from lab reagents and the environment. During childhood, black carbon particles may also be transported into the gut after mucociliary clearance of particles from the airways or systemic uptake after inhalation.[96–98] Once in the intestines, PM may alter bacterial growth by various mechanisms, such as gut inflammation, disruption of tight junction proteins, and oxidative stress.[99–102] The majority of these mechanisms have been exclusively investigated in *in vitro* studies and *in vivo* animal models. For instance, Mutlu et al. showed that exposure to high doses of urban airborne PM was associated with *a*) oxidant-dependent gastrointestinal epithelial cell death, *b*) disruption of the tight junction protein Zonula occludens-1, *c*) an increase in the inflammatory markers interleukin-6, nuclear factor-kappa B, and tumor necrosis factor α, and *d*) an increase in gut permeability in *in vitro* (Caco-2 intestinal epithelial barrier model) and *in vivo* animal (male C57BL/6 mice) models.[100,101] In addition, 126/SvEv mice gavaged with PM_{10} particles for 2 wk showed increased pro-inflammatory cytokine levels in intestinal tissue.[99] As mentioned previously,

Table 3. Overview of the associations between the bacterial Chao1 richness and Shannon and Simpson diversity indices and placental, cord blood, and urinary BC load.

	Placental BC ($n=63$)		Cord blood BC ($n=80$)		Urinary BC ($n=80$)	
	Percentage change	*p*-Value	Percentage change	*p*-Value	Percentage change	*p*-Value
Chao1 index	−6.63 (−17.02, 5.08)	0.26	0.52 (−9.18, 11.26)	0.92	−2.45 (−8.95, 4.51)	0.48
Shannon index	−4.38 (−8.31, −0.28)	0.04	−3.38 (−5.66, −0.84)	0.05	−3.39 (−5.77, −0.94)	0.009
Simpson index	−0.90 (−1.76, −0.04)	0.04	−0.91 (−1.66, −0.16)	0.02	−0.89 (−1.37, −0.40)	<0.0001

Note: Effects are expressed as percentage change and 95% CI for a doubling in black carbon load. Robust linear regression models were adjusted for parity, season of delivery, sequencing batch, age, sex, weight, and height of the child, and maternal education per categories included in Table 1. Urinary black carbon is normalized for osmolality. Participants were enrolled in the ENVIR*ON*AGE birth cohort. BC, black carbon; CI, confidence interval; ENVIR*ON*AGE, ENVIRonmental influence *ON* early AGEing birth cohort.

Table 4. Overview of the results of multiexposure models considering the associations between the bacterial Chao1 richness and Shannon and Simpson diversity indices and both the cord blood and urinary BC load.

	Cord blood BC ($n=76$)		Urine BC ($n=76$)	
	Percentage change	p-Value	Percentage change	p-Value
Chao1 index	1.62 (−8.19, 12.48)	0.76	−1.61 (−8.25, 5.50)	0.65
Shannon index	−2.61 (−6.17, 1.10)	0.16	−3.51 (−5.95, −1.00)	0.006
Simpson index	−0.85 (−1.59, −0.10)	0.03	−1.05 (−1.56, −0.54)	<0.0001

Note: Effects are expressed as percentage change and 95% CI for a doubling in BC load. Robust linear regression models were adjusted for parity, season of delivery, sequencing batch, age, sex, weight and height of the child, and maternal education per categories included in Table 1. Urinary black carbon is normalized for osmolality. In addition, $n=76$ because either only cord blood or urine was available for four participants. Participants were enrolled in the ENVIR*ON*AGE birth cohort. BC, black carbon; CI, confidence interval; ENVIR*ON*AGE, ENVIRonmental influence *ON* early AGEing birth cohort.

black carbon particles are formed during the incomplete combustion of carbonaceous fuels,[3,4] during which hazardous substances such as PAHs, including benzo(a)pyrene (BaP), can adhere to their surface. Besides a possible mutagenic and carcinogenic potential, multiple studies also reported a pro-inflammatory potential for BaP, potentially affecting intestinal bacterial growth.[103,104] For instance, Khalil et al. demonstrated a significant increase in murine intestinal inflammation in association with a high-fat diet following BaP exposure.[104] Additionally, C57BL/6 mice orally exposed to BaP showed a significant increment in inflammatory cell proliferation and crypt damage, leading to decreased levels of the intestinal bacterial genus *Lactobacillus*.[103]

To our knowledge, this study is the first to investigate the correlation between airborne particulate matter exposure of healthy young children during susceptible life periods and their gut bacterial richness and diversity of specific bacterial taxa. Other epidemiological studies examining the association between air pollution and the intestinal microbiome so far made use of spatial temporal modeled data.[24–53] These air pollution models only consider exposure at the residential address, implying that individual and time-activity mobility patterns, e.g., commuting, hobbies, and work, are not considered. Consequently, exposure misclassification and a potential underestimation of the health risk can occur.[6] As seen in our study, modeled black carbon exposure during pregnancy and the month, 6 months, or year before stool sample collection was not associated with the bacterial richness and diversity of the intestinal microbiome. To overcome these shortcomings, we employed the white light technique to assess individual and internal black carbon loads. The implication of this technique in population-based research is unique, allows the determination of a precise personal exposure measurement, and enables direct linkage with observed gut microbiome changes.[32]

We acknowledge some study limitations. First, only 85 children were included in the present study, resulting in a small sample size. Despite the small sample size, we were able to find statistically significant correlations and associations with diversity indices and the relative abundance of specific bacterial families. Due to the limited sample size of our study, our study population might not be completely representative for the general population: e.g., our study included only one mother giving birth via a cesarean section and had a slightly lower percentage of children of non-European descent (3.5% vs. 10.2%) and of mothers with low education levels (2.4% vs. 10.6%) in comparison with the entire birth cohort (Table S4). Moreover, the small sample size significantly limited our ability to test the influence of certain factors (e.g., cesarean section and descent) on the intestinal microbiome. Second, limited information regarding diet was available. Yet, we adjusted the robust linear regression models for self-reported fruit, vegetable, and soda intake, which did not significantly change our findings. Future population-based research is necessary to examine potential pathways (e.g., systemic oxidative stress and gut inflammation) that might underlie the observed associations between air pollution exposure and the intestinal microbiome because for now only *in vivo* animal and *in vitro* studies exist. In addition, metagenomic shotgun and pathway analyses could be performed to acquire more in-depth information on the microbiome composition and functionality.

Conclusion

Higher accumulation of black carbon particles in placental tissue, cord blood, and urine as internal biomarkers of prenatal and postnatal combustion-related air pollution exposure was associated with changes in intestinal bacterial diversity in young children. Black carbon loads in placental tissue were negatively associated

Table 5. Results of the relative abundance analysis examining the association between placental, cord blood and urinary BC and bacterial families computed with the ANCOM-BC R package.

Matrix	Family	p-Value	q-Value	Percentage difference
Placenta	*Anaerovoracaceae*	0.02	0.29	−45.81
Placenta	*Christenellaceae*	0.04	0.36	−85.18
Placenta	*Defluviitaleaceae*	0.003	0.09	−73.70
Placenta	*Marinifilaceae*	0.001	0.08	−96.92
Placenta	*Muribaculaceae*	0.02	0.29	−96.03
Placenta	*Oscillospiraceae*	0.009	0.21	−52.02
Cord blood	*Anaerovoraceae*	0.05	0.54	−45.81
Cord blood	*Coriobacteriaceae*	0.03	0.58	445.66
Urine	*Christensenellaceae*	0.0005	0.03	−85.84
Urine	*Coriobacteriaceae*	0.0003	0.08	−80.67
Urine	*Coriobacteriales incertae sedis*	0.05	0.42	−48.14
Urine	*Enterobacteriaceae*	0.05	0.42	233.09
Urine	*Methanobacteriaceae*	0.05	0.42	−57.80
Urine	*Rikenellaceae*	0.05	0.42	−59.88

Note: Only bacterial families with a $p \leq 0.05$ are shown. Results are expressed as percentage change per doubling in BC load: for instance, a −45.81% change would mean a 0.46-fold decrease per doubling in BC load. ANCOM-BC log-log models were corrected for parity, season of delivery, batch, age, sex, weight, height of the child, and maternal education per categories included in Table 1. Urinary black carbon was normalized for osmolality. $p \leq 0.05$ and $q \leq 0.10$ are considered statistically significant. Families that remained statistically significant after multiple testing correction via the false discovery rate are indicated in gray. Participants were enrolled in the ENVIR*ON*AGE birth cohort. Placenta $n=63$, cord blood $n=80$, and urine $n=80$. BC, black carbon; ENVIR*ON*AGE, ENVIRonmental influence ON early AGEing birth cohort.

with *Defluviitaleaceae* and *Marinifilaceae*, whereas urinary black carbon was negatively associated with *Christensenellaceae* and *Coriobacteriaceae*. These findings address the influential role of exposure to air pollution during pregnancy and early life in human health. Future studies are necessary to examine the mechanisms underlying the observed associations.

Acknowledgments

The authors thank all children and parents for taking part in the study and inviting them into their homes. The authors thank J.D.V.H. and B. McAmmond for sequencing data. This investigation is supported by the European Union research council Project ENVIRONAGE (ERC-2012-StG 310,890), Flemish Scientific Fund (G073315N/G048420N), and Methusalem T.V.P. holds a doctoral fellowship of the Research Foundation Flanders (FWO), grant number: 11C7421N.

References

1. Landrigan PJ, Fuller R, Acosta NJR, Adeyi O, Arnold R, Basu NN, et al. 2018. The *Lancet* Commission on pollution and health. Lancet 391(10119):462–512, PMID: 29056410, https://doi.org/10.1016/S0140-6736(17)32345-0.
2. European Union. 2008. Directive 2008/50/EC of the European Parliament and of the Council of 21 May 2008 on Ambient Air Quality and Cleaner Air for Europe, 169–212. https://eur-lex.europa.eu/legal-content/EN/TXT/HTML/?uri=CELEX:32008L0050&from=en [accessed 22 October 2021].
3. Janssen NA, Hoek G, Simic-Lawson M, Fischer P, van Bree L, ten Brink H, et al. 2011. Black carbon as an additional indicator of the adverse health effects of airborne particles compared with PM_{10} and $PM_{2.5}$. Environ Health Perspect 119(12):1691–1699, PMID: 21810552, https://doi.org/10.1289/ehp.1003369.
4. Niranjan R, Thakur AK. 2017. The toxicological mechanisms of environmental soot (black carbon) and carbon black: focus on oxidative stress and inflammatory pathways. Front Immunol 8:763, PMID: 28713383, https://doi.org/10.3389/fimmu.2017.00763.
5. Chow JC, Watson JG, Mauderly JL, Costa DL, Wyzga RE, Vedal S, et al. 2006. Health effects of fine particulate air pollution: lines that connect. J Air Waste Manag Assoc 56(10):1368–1380, PMID: 17063860, https://doi.org/10.1080/10473289.2006.10464545.
6. Saenen ND, Bové H, Steuwe C, Roeffaers MBJ, Provost EB, Lefebvre W, et al. 2017. Children's urinary environmental carbon load. A novel marker reflecting residential ambient air pollution exposure? Am J Respir Crit Care Med 196(7):873–881, PMID: 28686472, https://doi.org/10.1164/rccm.201704-0797OC.
7. Bove H, Bongaerts E, Slenders E, Bijnens EM, Saenen ND, Gyselaers W, et al. 2019. Ambient black carbon particles reach the fetal side of human placenta. Nat Commun 10(1):3866, PMID: 31530803, https://doi.org/10.1038/s41467-019-11654-3.
8. Bongaerts E, Lecante LL, Bove H, Roeffaers MBJ, Ameloot M, Fowler PA, et al. 2022. Maternal exposure to ambient black carbon particles and their presence in maternal and fetal circulation and organs: an analysis of two independent population-based observational studies. Lancet Planet Health 6(10):e804–e811, PMID: 36208643, https://doi.org/10.1016/S2542-5196(22)00200-5.
9. Ursell LK, Metcalf JL, Parfrey LW, Knight R. 2012. Defining the human microbiome. Nutr Rev 70 (suppl 1):S38–S44, PMID: 22861806, https://doi.org/10.1111/j.1753-4887.2012.00493.x.
10. Mahowald MA, Rey FE, Seedorf H, Turnbaugh PJ, Fulton RS, Wollam A, et al. 2009. Characterizing a model human gut microbiota composed of members of its two dominant bacterial phyla. Proc Natl Acad Sci USA 106(14):5859–5864, PMID: 19321416, https://doi.org/10.1073/pnas.0901529106.
11. Derrien M, Alvarez AS, de Vos WM. 2019. The gut microbiota in the first decade of life. Trends Microbiol 27(12):997–1010, PMID: 31474424, https://doi.org/10.1016/j.tim.2019.08.001.
12. Ventura M, O'Toole PW, de Vos WM, van Sinderen D. 2018. Selected aspects of the human gut microbiota. Cell Mol Life Sci 75(1):81–82, PMID: 28986602, https://doi.org/10.1007/s00018-017-2669-8.
13. Jandhyala SM, Talukdar R, Subramanyam C, Vuyyuru H, Sasikala M, Reddy DN. 2015. Role of the normal gut microbiota. World J Gastroenterol 21(29):8787–8803, PMID: 26269668, https://doi.org/10.3748/wjg.v21.i29.8787.
14. Abdellatif AM, Sarvetnick NE. 2019. Current understanding of the role of gut dysbiosis in type 1 diabetes. J Diabetes 11(8):632–644, PMID: 30864231, https://doi.org/10.1111/1753-0407.12915.
15. Amabebe E, Robert FO, Agbalalah T, Orubu ESF. 2020. Microbial dysbiosis-induced obesity: role of gut microbiota in homoeostasis of energy metabolism. Br J Nutr 123(10):1127–1137, PMID: 32008579, https://doi.org/10.1017/S0007114520000380.
16. Proctor C, Thiennimitr P, Chattipakorn N, Chattipakorn SC. 2017. Diet, gut microbiota and cognition. Metab Brain Dis 32(1):1–17, PMID: 27709426, https://doi.org/10.1007/s11011-016-9917-8.
17. Yang T, Santisteban MM, Rodriguez V, Li E, Ahmari N, Carvajal JM, et al. 2015. Gut dysbiosis is linked to hypertension. Hypertension 65(6):1331–1340, PMID: 25870193, https://doi.org/10.1161/HYPERTENSIONAHA.115.05315.
18. Bajinka O, Tan Y, Abdelhalim KA, Özdemir G, Qiu X. 2020. Extrinsic factors influencing gut microbes, the immediate consequences and restoring eubiosis. AMB Express 10(1):130, PMID: 32710186, https://doi.org/10.1186/s13568-020-01066-8.
19. Haro C, Rangel-Zúñiga OA, Alcalá-Díaz JF, Gómez-Delgado F, Pérez-Martínez P, Delgado-Lista J, et al. 2016. Intestinal microbiota is influenced by gender and body mass index. PLoS One 11(5):e0154090, PMID: 27228093, https://doi.org/10.1371/journal.pone.0154090.
20. Lewis CR, Bonham KS, McCann SH, Volpe AR, D'Sa V, Naymik M, et al. 2021. Family SES is associated with the gut microbiome in infants and children. Microorganisms 9(8):1608, PMID: 34442687, https://doi.org/10.3390/microorganisms9081608.
21. Falony G, Joossens M, Vieira-Silva S, Wang J, Darzi Y, Faust K, et al. 2016. Population-level analysis of gut microbiome variation. Science 352(6285):560–564, PMID: 27126039, https://doi.org/10.1126/science.aad3503.
22. Valles Y, Francino MP. 2018. Air pollution, early life microbiome, and development. Curr Environ Health Rep 5(4):512–521, PMID: 30269309, https://doi.org/10.1007/s40572-018-0215-y.
23. Mariani J, Favero C, Spinazze A, Cavallo DM, Carugno M, Motta V, et al. 2018. Short-term particulate matter exposure influences nasal microbiota in a population of healthy subjects. Environ Res 162:119–126, PMID: 29291434, https://doi.org/10.1016/j.envres.2017.12.016.
24. Zheng P, Zhang B, Zhang K, Lv X, Wang Q, Bai X. 2020. The Impact of air pollution on intestinal microbiome of asthmatic children: a panel study. Biomed Res Int 2020:5753427, PMID: 33204702, https://doi.org/10.1155/2020/5753427.
25. Alderete TL, Jones RB, Chen Z, Kim JS, Habre R, Lurmann F, et al. 2018. Exposure to traffic-related air pollution and the composition of the gut microbiota in overweight and obese adolescents. Environ Res 161:472–478, PMID: 29220800, https://doi.org/10.1016/j.envres.2017.11.046.
26. Liu T, Chen X, Xu Y, Wu W, Tang W, Chen Z, et al. 2019. Gut microbiota partially mediates the effects of fine particulate matter on type 2 diabetes: evidence from a population-based epidemiological study. Environ Int 130:104882, PMID: 31202028, https://doi.org/10.1016/j.envint.2019.05.076.
27. Janssen BG, Madhloum N, Gyselaers W, Bijnens E, Clemente DB, Cox B, et al. 2017. Cohort Profile: the ENVIRonmental Influence on Early AGEing (ENVIR*ON*AGE): a birth cohort study. Int J Epidemiol 46(5):1386–1387, PMID: 28089960, https://doi.org/10.1093/ije/dyw269.
28. Martens DS, Cox B, Janssen BG, Clemente DBP, Gasparrini A, Vanpoucke C, et al. 2017. Prenatal air pollution and newborns' predisposition to accelerated biological aging. JAMA Pediatr 171(12):1160–1167, PMID: 29049509, https://doi.org/10.1001/jamapediatrics.2017.3024.
29. Martens DS, Janssen BG, Bijnens EM, Clemente DBP, Vineis P, Plusquin M, et al. 2020. Association of parental socioeconomic status and newborn telomere length. JAMA Netw Open 3(5):e204057, PMID: 32364595, https://doi.org/10.1001/jamanetworkopen.2020.4057.
30. Saenen ND, Vrijens K, Janssen BG, Roels HA, Neven KY, Vanden Berghe W, et al. 2017. Lower Placental leptin promoter methylation in association with fine particulate matter air pollution during pregnancy and placental nitrosative stress at birth in the ENVIRONAGE cohort. Environ Health Perspect 125(2):262–268, PMID: 27623604, https://doi.org/10.1289/EHP38.
31. Martens DS, Gouveia S, Madhloum N, Janssen BG, Plusquin M, Vanpoucke C, et al. 2017. Neonatal cord blood oxylipins and exposure to particulate matter in the early-life environment: an ENVIR*ON*AGE birth cohort study. Environ Health Perspect 125(4):691–698, PMID: 27814242, https://doi.org/10.1289/EHP291.
32. Bove H, Steuwe C, Fron E, Slenders E, D'Haen J, Fujita Y, et al. 2016. Biocompatible label-free detection of carbon black particles by femtosecond pulsed laser microscopy. Nano Lett 16(5):3173–3178, PMID: 27104759, https://doi.org/10.1021/acs.nanolett.6b00502.
33. Lefebvre W, Vercauteren J, Schrooten L, Janssen S, Degraeuwe B, Maenhaut W, et al. 2011. Validation of the MIMOSA-AURORA-IFDM model chain for policy support: modeling concentrations of elemental carbon in Flanders. Atmos Environ 45(37):6705–6713, https://doi.org/10.1016/j.atmosenv.2011.08.033.
34. Thomas V, Clark J, Dore J. 2015. Fecal microbiota analysis: an overview of sample collection methods and sequencing strategies. Future Microbiol 10(9):1485–504, PMID: 26347019, https://doi.org/10.2217/fmb.15.87.
35. Callahan BJ, McMurdie PJ, Rosen MJ, Han AW, Johnson AJ, Holmes SP. 2016. DADA2: high-resolution sample inference from Illumina amplicon data. Nat Methods 13(7):581–583, PMID: 27214047, https://doi.org/10.1038/nmeth.3869.

36. Quast C, Pruesse E, Yilmaz P, Gerken J, Schweer T, Yarza P, et al. 2013. The SILVA ribosomal RNA gene database project: improved data processing and web-based tools. Nucleic Acids Res 41(Database issue):D590–D596, PMID: 23193283, https://doi.org/10.1093/nar/gks1219.
37. Yilmaz P, Parfrey LW, Yarza P, Gerken J, Pruesse E, Quast C, et al. 2014. The SILVA and "all-species living tree project (LTP)" taxonomic frameworks. Nucleic Acids Res 42(Database issue):D643–D648, PMID: 24293649, https://doi.org/10.1093/nar/gkt1209.
38. Wright ES. 2016. Using DECIPHER v2.0 to analyze big biological sequence data in R. R J 8(1):352–359, https://doi.org/10.32614/RJ-2016-025.
39. McMurdie PJ, Holmes S. 2013. Phyloseq: an R package for reproducible interactive analysis and graphics of microbiome census data. PLoS One 8(4): e61217, PMID: 23630581, https://doi.org/10.1371/journal.pone.0061217.
40. Davis NM, Proctor DM, Holmes SP, Relman DA, Callahan BJ. 2018. Simple statistical identification and removal of contaminant sequences in marker-gene and metagenomics data. Microbiome 6(1):226, PMID: 30558668, https://doi.org/10.1186/s40168-018-0605-2.
41. Kandlikar GS, Gold ZJ, Cowen MC, Meyer RS, Freise AC, Kraft NJB, et al. 2018. Ranacapa: an R package and Shiny web app to explore environmental DNA data with exploratory statistics and interactive visualizations. F1000Res 7:1734, PMID: 30613396, https://doi.org/10.12688/f1000research.16680.1.
42. Kim BR, Shin J, Guevarra R, Lee JH, Kim DW, Seol KH, et al. 2017. Deciphering diversity indices for a better understanding of microbial communities. J Microbiol Biotechnol 27(12):2089–2093, PMID: 29032640, https://doi.org/10.4014/jmb.1709.09027.
43. Berry ASF, Pierdon MK, Misic AM, Sullivan MC, O'Brien K, Chen Y, et al. 2021. Remodeling of the maternal gut microbiome during pregnancy is shaped by parity. Microbiome 9(1):146, PMID: 34176489, https://doi.org/10.1186/s40168-021-01089-8.
44. Chen R, Peng RD, Meng X, Zhou Z, Chen B, Kan H. 2013. Seasonal variation in the acute effect of particulate air pollution on mortality in the China Air Pollution and Health Effects Study (CAPES). Sci Total Environ 450–451:259–265, PMID: 23500824, https://doi.org/10.1016/j.scitotenv.2013.02.040.
45. Wang Y, LêCao KA. 2020. Managing batch effects in microbiome data. Brief Bioinform 21(6):1954–1970, PMID: 31776547, https://doi.org/10.1093/bib/bbz105.
46. Bosco N, Noti M. 2021. The aging gut microbiome and its impact on host immunity. Genes Immun 22(5–6):289–303, PMID: 33875817, https://doi.org/10.1038/s41435-021-00126-8.
47. Valeri F, Endres K. 2021. How biological sex of the host shapes its gut microbiota. Front Neuroendocrinol 61:100912, PMID: 33713673, https://doi.org/10.1016/j.yfrne.2021.100912.
48. Sepp E, Loivukene K, Julge K, Voor T, Mikelsaar M. 2013. The association of gut microbiota with body weight and body mass index in preschool children of Estonia. Microb Ecol Health Dis 24(1), PMID: 24009544, https://doi.org/10.3402/mehd.v24i0.19231.
49. Manor O, Dai CL, Kornilov SA, Smith B, Price ND, Lovejoy JC, et al. 2020. Health and disease markers correlate with gut microbiome composition across thousands of people. Nat Commun 11(1):5206, PMID: 33060586, https://doi.org/10.1038/s41467-020-18871-1.
50. Wang Y, Wang Y, Xu H, Zhao Y, Marshall JD. 2022. Ambient air pollution and socioeconomic status in China. Environ Health Perspect 130(6):67001, PMID: 35674427, https://doi.org/10.1289/EHP9872.
51. Ballon M, Botton J, Charles MA, Carles S, de Lauzon-Guillain B, Forhan A, et al. 2018. Socioeconomic inequalities in weight, height and body mass index from birth to 5 years. Int J Obes (Lond) 42(9):1671–1679, PMID: 30120430, https://doi.org/10.1038/s41366-018-0180-4.
52. Sherar LB, Griffin TP, Ekelund U, Cooper AR, Esliger DW, van Sluijs EM, et al. 2016. Association between maternal education and objectively measured physical activity and sedentary time in adolescents. J Epidemiol Community Health 70(6):541–548, PMID: 26802168, https://doi.org/10.1136/jech-2015-205763.
53. Fouladi F, Bailey MJ, Patterson WB, Sioda M, Blakley IC, Fodor AA, et al. 2020. Air pollution exposure is associated with the gut microbiome as revealed by shotgun metagenomic sequencing. Environ Int 138:105604, PMID: 32135388, https://doi.org/10.1016/j.envint.2020.105604.
54. Reyman M, van Houten MA, van Baarle D, Bosch A, Man WH, Chu M, et al. 2019. Impact of delivery mode-associated gut microbiota dynamics on health in the first year of life. Nat Commun 10(1):4997, PMID: 31676793, https://doi.org/10.1038/s41467-019-13014-7.
55. McLean C, Jun S, Kozyrskyj A. 2019. Impact of maternal smoking on the infant gut microbiota and its association with child overweight: a scoping review. World J Pediatr 15(4):341–349, PMID: 31290060, https://doi.org/10.1007/s12519-019-00278-8.
56. Zou ZH, Liu D, Li HD, Zhu DP, He Y, Hou T, et al. 2018. Prenatal and postnatal antibiotic exposure influences the gut microbiota of preterm infants in neonatal intensive care units. Ann Clin Microbiol Antimicrob 17(1):9, PMID: 29554907, https://doi.org/10.1186/s12941-018-0264-y.
57. Berkowitz L, Pardo-Roa C, Salazar GA, Salazar-Echegarai F, Miranda JP, Ramirez G, et al. 2019. Mucosal exposure to cigarette components induces intestinal inflammation and alters antimicrobial response in mice. Front Immunol 10:2289, PMID: 31608070, https://doi.org/10.3389/fimmu.2019.02289.
58. Ramirez J, Guarner F, Fernandez LB, Maruy A, Sdepanian VL, Cohen H. 2020. Antibiotics as major disruptors of gut microbiota. Front Cell Infect Microbiol 10:572912, PMID: 33330122, https://doi.org/10.3389/fcimb.2020.572912.
59. Dwiyanto J, Hussain MH, Reidpath D, Ong KS, Qasim A, Lee SWH, et al. 2021. Ethnicity influences the gut microbiota of individuals sharing a geographical location: a cross-sectional study from a middle-income country. Sci Rep 11(1):2618, PMID: 33514807, https://doi.org/10.1038/s41598-021-82311-3.
60. Thompson AL. 2012. Developmental origins of obesity: early feeding environments, infant growth, and the intestinal microbiome. Am J Hum Biol 24(3):350–360, PMID: 22378322, https://doi.org/10.1002/ajhb.22254.
61. Singh RK, Chang HW, Yan D, Lee KM, Ucmak D, Wong K, et al. 2017. Influence of diet on the gut microbiome and implications for human health. J Transl Med 15(1):73, PMID: 28388917, https://doi.org/10.1186/s12967-017-1175-y.
62. Bowyer RCE, Jackson MA, Le Roy CI, Ni Lochlainn M, Spector TD, Dowd JB, et al. 2019. Socioeconomic status and the gut microbiome: a TwinsUK cohort study. Microorganisms 7(1):17, PMID: 30641975, https://doi.org/10.3390/microorganisms7010017.
63. Lin H, Peddada SD. 2020. Analysis of compositions of microbiomes with bias correction. Nat Commun 11(1):3514, PMID: 32665548, https://doi.org/10.1038/s41467-020-17041-7.
64. Calle ML. 2019. Statistical analysis of metagenomics data. Genomics Inform 17(1):e6, PMID: 30929407, https://doi.org/10.5808/GI.2019.17.1.e6.
65. Dogra SK, Dore J, Damak S. 2020. Gut microbiota resilience: definition, link to health and strategies for intervention. Front Microbiol 11:572921, PMID: 33042082, https://doi.org/10.3389/fmicb.2020.572921.
66. Liu Y, Song X, Zhou H, Zhou X, Xia Y, Dong X, et al. 2018. Gut microbiome associates with lipid-lowering effect of rosuvastatin in vivo. Front Microbiol 9:530, PMID: 29623075, https://doi.org/10.3389/fmicb.2018.00530.
67. Warbeck C, Dowd AJ, Kronlund L, Parmar C, Daun JT, Wytsma-Fisher K, et al. 2021. Feasibility and effects on the gut microbiota of a 12-week high-intensity interval training plus lifestyle education intervention on inactive adults with celiac disease. Appl Physiol Nutr Metab 46(4):325–336, PMID: 32961065, https://doi.org/10.1139/apnm-2020-0459.
68. Ge XD, Chang CE, Chen HL, Liu TT, Chen LG, Huang Y, et al. 2020. Luteolin cooperated with metformin hydrochloride alleviates lipid metabolism disorders and optimizes intestinal flora compositions of high-fat diet mice. Food Funct 11(11):10033–10046, PMID: 33135040, https://doi.org/10.1039/d0fo01840f.
69. Kwan SY, Jiao J, Joon A, Wei P, Petty LE, Below JE, et al. 2022. Gut microbiome features associated with liver fibrosis in Hispanics, a population at high risk for fatty liver disease. Hepatology 75(4):955–967, PMID: 34633706, https://doi.org/10.1002/hep.32197.
70. Waters JL, Ley RE. 2019. The human gut bacteria Christensenellaceae are widespread, heritable, and associated with health. BMC Biol 17(1):, PMID: 31660948, https://doi.org/10.1186/s12915-019-0699-4.
71. Pascal V, Pozuelo M, Borruel N, Casellas F, Campos D, Santiago A, et al. 2017. A microbial signature for Crohn's disease. Gut 66(5):813–822, PMID: 28179361, https://doi.org/10.1136/gutjnl-2016-313235.
72. Lee T, Clavel T, Smirnov K, Schmidt A, Lagkouvardos I, Walker A, et al. 2017. Oral versus intravenous iron replacement therapy distinctly alters the gut microbiota and metabolome in patients with IBD. Gut 66(5):863–871, PMID: 26848182, https://doi.org/10.1136/gutjnl-2015-309940.
73. Pittayanon R, Lau JT, Leontiadis GI, Tse F, Yuan Y, Surette M, et al. 2020. Differences in gut microbiota in patients with vs without inflammatory bowel diseases: a systematic review. Gastroenterology 158(4):930–946.e1, PMID: 31812509, https://doi.org/10.1053/j.gastro.2019.11.294.
74. Zhao X, Zhang Z, Hu B, Huang W, Yuan C, Zou L. 2018. Response of gut microbiota to metabolite changes induced by endurance exercise. Front Microbiol 9:765, PMID: 29731746, https://doi.org/10.3389/fmicb.2018.00765.
75. Clavel TLP, Charrier C. 2014. The Family *Coriobacteriaceae*. In: *The Prokaryotes*. Rosenberg E, DeLong EF, Lory S, Stackebrandt E, Thompson F, eds. Berlin, Germany: Springer, https://doi.org/10.1007/978-3-642-30138-4_343.
76. Liu H, Zhang H, Wang X, Yu X, Hu C, Zhang X. 2018. The family *Coriobacteriaceae* is a potential contributor to the beneficial effects of Roux-en-Y gastric bypass on type 2 diabetes. Surg Obes Relat Dis 14(5):584–593, PMID: 29459013, https://doi.org/10.1016/j.soard.2018.01.012.
77. Goodrich JK, Waters JL, Poole AC, Sutter JL, Koren O, Blekhman R, et al. 2014. Human genetics shape the gut microbiome. Cell 159(4):789–799, PMID: 25417156, https://doi.org/10.1016/j.cell.2014.09.053.
78. Fu J, Bonder MJ, Cenit MC, Tigchelaar EF, Maatman A, Dekens JA, et al. 2015. The Gut microbiome contributes to a substantial proportion of the variation in blood lipids. Circ Res 117(9):817–824, PMID: 26358192, https://doi.org/10.1161/CIRCRESAHA.115.306807.

79. He Y, Wu W, Wu S, Zheng HM, Li P, Sheng HF, et al. 2018. Linking gut microbiota, metabolic syndrome and economic status based on a population-level analysis. Microbiome 6(1):172, PMID: 30249275, https://doi.org/10.1186/s40168-018-0557-6.
80. Li X, Zhang X, Zhang Z, Han L, Gong D, Li J, et al. 2019. Air pollution exposure and immunological and systemic inflammatory alterations among schoolchildren in China. Sci Total Environ 657:1304–1310, PMID: 30677897, https://doi.org/10.1016/j.scitotenv.2018.12.153.
81. Tamagawa E, Bai N, Morimoto K, Gray C, Mui T, Yatera K, et al. 2008. Particulate matter exposure induces persistent lung inflammation and endothelial dysfunction. Am J Physiol Lung Cell Mol Physiol 295(1):L79–L85, PMID: 18469117, https://doi.org/10.1152/ajplung.00048.2007.
82. Gómez-Hurtado I, Santacruz A, Peiró G, Zapater P, Gutiérrez A, Pérez-Mateo M, et al. 2011. Gut microbiota dysbiosis is associated with inflammation and bacterial translocation in mice with CCl4-induced fibrosis. PLoS One 6(7): e23037, PMID: 21829583, https://doi.org/10.1371/journal.pone.0023037.
83. Xu W, Song Q. 2017. Abstract 19614: C-reactive protein re-shapes the composition of gut microbiota and causes obesity. Circulation 136(suppl 1):A19614, https://doi.org/10.1161/circ.136.suppl_1.19614.
84. Armstrong H, Bording-Jorgensen M, Dijk S, Wine E. 2018. The complex interplay between chronic inflammation, the microbiome, and cancer: understanding disease progression and what we can do to prevent it. Cancers (Basel). 10(3):83, PMID: 29558443, https://doi.org/10.3390/cancers10030083.
85. Xu Y, Li Z, Liu Y, Pan B, Peng R, Shao W, et al. 2021. Differential roles of water-insoluble and water-soluble fractions of diesel exhaust particles in the development of adverse health effects due to chronic instillation of diesel exhaust particles. Chem Res Toxicol 34(12):2450–2459, PMID: 34780166, https://doi.org/10.1021/acs.chemrestox.1c00199.
86. Boyle AK, Rinaldi SF, Norman JE, Stock SJ. 2017. Preterm birth: inflammation, fetal injury and treatment strategies. J Reprod Immunol 119:62–66, PMID: 28122664, https://doi.org/10.1016/j.jri.2016.11.008.
87. Perez-Muñoz ME, Arrieta MC, Ramer-Tait AE, Walter J. 2017. A critical assessment of the "sterile womb" and "in utero colonization" hypotheses: implications for research on the pioneer infant microbiome. Microbiome 5(1):48, PMID: 28454555, https://doi.org/10.1186/s40168-017-0268-4.
88. Dunn AB, Jordan S, Baker BJ, Carlson NS. 2017. The maternal infant microbiome: considerations for labor and birth. MCN Am J Matern Child Nurs 42(6):318–325, PMID: 28825919, https://doi.org/10.1097/NMC.0000000000000373.
89. Backhed F, Roswall J, Peng Y, Feng Q, Jia H, Kovatcheva-Datchary P, et al. 2015. Dynamics and stabilization of the human gut microbiome during the first year of life. Cell Host Microbe 17(5):690–703, PMID: 25974306, https://doi.org/10.1016/j.chom.2015.04.004.
90. Moossavi S, Miliku K, Sepehri S, Khafipour E, Azad MB. 2018. The prebiotic and probiotic properties of human milk: implications for infant immune development and pediatric asthma. Front Pediatr 6:197, PMID: 30140664, https://doi.org/10.3389/fped.2018.00197.
91. Collado MC, Rautava S, Aakko J, Isolauri E, Salminen S. 2016. Human gut colonisation may be initiated in utero by distinct microbial communities in the placenta and amniotic fluid. Sci Rep 6:23129, PMID: 27001291, https://doi.org/10.1038/srep23129.
92. Funkhouser LJ, Bordenstein SR. 2013. Mom knows best: the universality of maternal microbial transmission. PLoS Biol 11(8):e1001631, PMID: 23976878, https://doi.org/10.1371/journal.pbio.1001631.
93. Jiménez E, Marín ML, Martín R, Odriozola JM, Olivares M, Xaus J, et al. 2008. Is meconium from healthy newborns actually sterile? Res Microbiol 159(3):187–193, PMID: 18281199, https://doi.org/10.1016/j.resmic.2007.12.007.
94. Dos Santos SJ, Pakzad Z, Elwood CN, Albert AYK, Gantt S, Manges AR, et al. 2021. Early neonatal meconium does not have a demonstrable microbiota determined through use of robust negative controls with *cpn*60-based microbiome profiling. Microbiol Spectr 9(2):e0006721, PMID: 34585952, https://doi.org/10.1128/Spectrum.00067-21.
95. Kennedy KM, Gerlach MJ, Adam T, Heimesaat MM, Rossi L, Surette MG, et al. 2021. Fetal meconium does not have a detectable microbiota before birth. Nat Microbiol 6(7):865–873, PMID: 33972766, https://doi.org/10.1038/s41564-021-00904-0.
96. Beamish LA, Osornio-Vargas AR, Wine E. 2011. Air pollution: an environmental factor contributing to intestinal disease. J Crohns Colitis 5(4):279–286, PMID: 21683297, https://doi.org/10.1016/j.crohns.2011.02.017.
97. Bosch AJT, Rohm TV, Alasfoor S, Dervos T, Cavelti-Weder C. 2018. Air pollution–induced diabetes is mediated via the gastrointestinal tract. Diabetes 67(suppl 1):2416–PUB, https://doi.org/10.2337/db18-2416-PUB.
98. Salim SY, Kaplan GG, Madsen KL. 2014. Air pollution effects on the gut microbiota: a link between exposure and inflammatory disease. Gut Microbes 5(2):215–219, PMID: 24637593, https://doi.org/10.4161/gmic.27251.
99. Kish L, Hotte N, Kaplan GG, Vincent R, Tso R, Gänzle M, et al. 2013. Environmental particulate matter induces murine intestinal inflammatory responses and alters the gut microbiome. PLoS One 8(4):e62220, PMID: 23638009, https://doi.org/10.1371/journal.pone.0062220.
100. Mutlu EA, Comba IY, Cho T, Engen PA, Yazici C, Soberanes S, et al. 2018. Inhalational exposure to particulate matter air pollution alters the composition of the gut microbiome. Environ Pollut 240:817–830, PMID: 29783199, https://doi.org/10.1016/j.envpol.2018.04.130.
101. Mutlu EA, Engen PA, Soberanes S, Urich D, Forsyth CB, Nigdelioglu R, et al. 2011. Particulate matter air pollution causes oxidant-mediated increase in gut permeability in mice. Part Fibre Toxicol 8:19, PMID: 21658250, https://doi.org/10.1186/1743-8977-8-19.
102. Renwick AG, Drasar BS. 1976. Environmental carcinogens and large bowel cancer. Nature 263(5574):234–235, PMID: 958475, https://doi.org/10.1038/263234a0.
103. Ribiere C, Peyret P, Parisot N, Darcha C, Dechelotte PJ, Barnich N, et al. 2016. Oral exposure to environmental pollutant benzo[a]pyrene impacts the intestinal epithelium and induces gut microbial shifts in murine model. Sci Rep 6:31027, PMID: 27503127, https://doi.org/10.1038/srep31027.
104. Khalil A, Villard P-H, Dao MA, Burcelin R, Champion S, Fouchier F, et al. 2010. Polycyclic aromatic hydrocarbons potentiate high-fat diet effects on intestinal inflammation. Toxicol Lett 196(3):161–167, PMID: 20412841, https://doi.org/10.1016/j.toxlet.2010.04.010.